

# TransVFC: A Transformable Video Feature Compression Framework for Machines

Yuxiao Sun<sup>a,b</sup>, Yao Zhao<sup>a,b</sup>, Meiqin Liu<sup>a,b,\*</sup>, Chao Yao<sup>c</sup>, Huihui Bai<sup>a,b</sup>, Chunyu Lin<sup>a,b</sup>, Weisi Lin<sup>d</sup>

<sup>a</sup>*Institute of Information Science, Beijing Jiaotong University, Beijing, 100044, China*

<sup>b</sup>*Visual Intelligence +X International Cooperation Joint Laboratory of MOE, Beijing, 100044, China*

<sup>c</sup>*School of Computer and Communication Engineering, University of Science and Technology  
Beijing, Beijing, 100083, China*

<sup>d</sup>*School of Computer Science and Engineering, Nanyang Technological University, 639798, Singapore*

---

## Abstract

Nowadays, more and more video transmissions primarily aim at downstream machine vision tasks rather than humans. While widely deployed Human Visual System (HVS) oriented video coding standards like H.265/HEVC and H.264/AVC are efficient, they are not the optimal approaches for Video Coding for Machines (VCM) scenarios, leading to unnecessary bitrate expenditure. The academic and technical exploration within the VCM domain has led to the development of several strategies, and yet, conspicuous limitations remain in their adaptability for multi-task scenarios. To address the challenge, we propose a Transformable Video Feature Compression (TransVFC) framework. It offers a compress-then-transfer solution and includes a video feature codec and Feature Space Transform (FST) modules. In particular, the temporal redundancy of video features is squeezed by the codec through the scheme-based inter-prediction module. Then, the codec implements perception-guided conditional coding to minimize spatial redundancy and help the reconstructed features align with downstream machine perception. After that, the reconstructed features are transferred to new feature spaces for diverse downstream tasks by FST modules. To accommodate a new downstream task, it only requires training one lightweight FST

---

\*Corresponding author

*Email addresses:* 22110081@bjtu.edu.cn (Yuxiao Sun), yzhao@bjtu.edu.cn (Yao Zhao), mqliu@bjtu.edu.cn (Meiqin Liu), yaochao@ustb.edu.cn (Chao Yao), hhhbai@bjtu.edu.cn (Huihui Bai), cylin@bjtu.edu.cn (Chunyu Lin), wslin@ntu.edu.sg (Weisi Lin)

module, avoiding retraining and redeploying the upstream codec and downstream task networks. Experiments show that TransVFC achieves high rate-task performance for diverse tasks of different granularities. We expect our work can provide valuable insights for video feature compression in multi-task scenarios. The codes are at <https://github.com/Ws-Syx/TransVFC>.

*Keywords:* Neural video compression, Feature compression, Video coding for machines, Intermediate feature

---

## 1. Introduction

Digital video plays a crucial role in our lives, constituting a significant portion of daily information consumption. For videos aimed at the Human Visual System (HVS), such as movies and short clips, it is essential to preserve visual details perceptible to humans during compression. Meanwhile, videos collected for machine vision tasks, such as surveillance [1] and facial recognition [2], do not require maintaining all visual details [3, 4]. Currently, neural video compression frameworks for HVS have evolved significantly and offer excellent video compression performance [5, 6, 7]. However, the comprehensive exploration of neural-based Video Coding for Machines (VCM) remains nascent.

HVS-oriented video codecs, such as H.265/HEVC [9] and H.264/AVC [8], are frequently employed to compress videos for downstream analysis, as shown in Figure 1(a). However, these approaches encounter two limitations in VCM scenarios. Firstly, these compression frameworks focus on minimizing pixel-domain and HVS-related distortion (PSNR and MS-SSIM) rather than meeting the specific needs of machine vision applications, which is a sub-optimal approach for machine vision. Secondly, machine vision tasks usually require only a subset of image content [3, 15]. For example, indiscriminately transmitting the background for downstream image classification leads to bitrate wastage. There is a need for more tailored approaches in machine-centric scenarios.

Some researches delve into the Analyze-Then-Compress (ATC) paradigm to solve the above problems. The paradigm begins with feature extraction from images, fol-

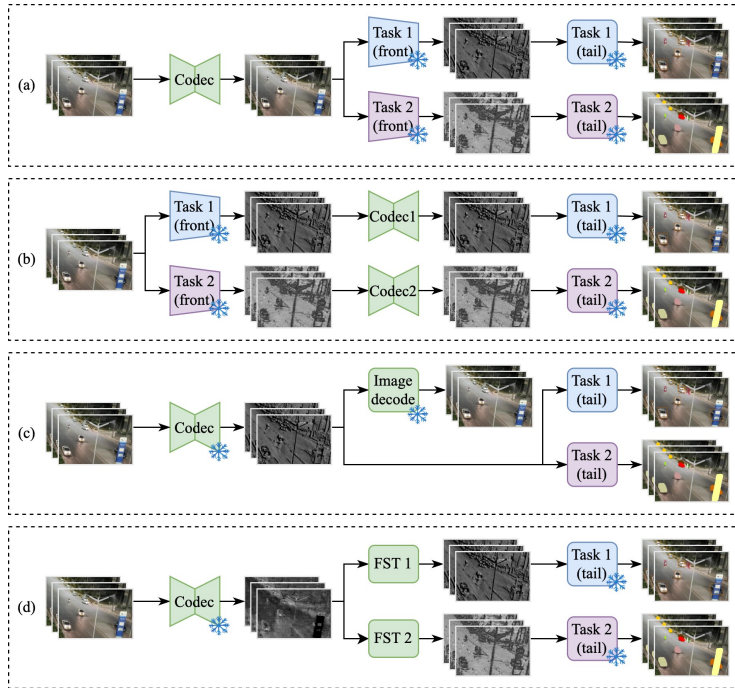


Figure 1: A comparison of different pipelines in VCM scenarios. “Task(front)” represents the shallow layers of the task network, “Task(tail)” denotes the rest part of the downstream network, and the snowflake symbol represents “frozen”. (a) Videos are compressed by a hybrid or neural-based codec [8, 9, 10, 11] and analyzed by downstream networks. (b) Intermediate features are extracted by the shallow layers of the task network and compressed by a specific-optimized video feature codec [12, 13]. (c) The intermediate features for frame reconstruction are used to perform machine vision tasks, and the whole downstream task network is optimized [14]. (d) Our framework uses a video feature codec for continuous feature transmission, then transfers features to various downstream tasks by lightweight Feature Space Transform (FST) modules.

lowed by feature compression for specific downstream tasks [16]. To enhance the versatility, some studies [3] focus on mining the generalization of intermediate features across various downstream tasks. Nonetheless, the above advancements only cater to intra-compression, not addressing the temporal redundancy in continuous features. For video feature compression, one strategy [12, 13] entails optimizing a video feature codec by the specific downstream loss, as shown in Figure 1(b). Alternatively, another strategy [14] focuses on freezing the codec while fine-tuning the entire downstream task network, as described in Figure 1(c). However, these approaches require retrain-

ing and redeploying either the upstream codec or downstream machine vision networks to accommodate new downstream tasks, thus costing more computation resources and limiting their scalability in real-world applications.

For better scalability and versatility in multi-task scenarios, we propose a Transformable Video Feature Compression (TransVFC) framework that offers a compress-then-transfer solution. As illustrated in Figure 1(d), our proposed framework contains an innovative neural-based video feature codec and diverse lightweight Feature Space Transform (FST) modules. In detail, The codec employs a scheme-based inter-prediction module to squeeze the temporal redundancy of video features and form a coarse compensated feature. Furthermore, it conducts perception-guided conditional coding for fine reconstruction and helps the reconstructed feature align with downstream machine perception. Subsequently, the reconstructed features are transferred to other feature spaces of diverse downstream machine vision tasks by FST modules. For any new downstream task, it only requires training one lightweight FST module, instead of retraining and redeploying the upstream codec or networks of downstream tasks. The experiments are conducted on three machine vision tasks of different granularities. The results demonstrate that the proposed TransVFC performs better than SOTA neural codecs on all downstream tasks, and outperforms VTM-23.1 [17] on video instance segmentation and object detection. The contributions are as follows:

- We propose a novel Transformable Video Feature Compression (TransVFC) framework. It comprises two components: a video features codec and diverse feature space transform modules, offering a scalable and deployable VCM solution.
- We introduce an innovative neural-based video feature codec to squeeze redundancy in the feature domain. It includes a scheme-based inter-prediction module and a perception-guided conditional coding module.
- We design the lightweight Feature Space Transform module that transfers intermediate features to diverse downstream tasks in a highly scalable way. Experimental results validate the scalability and effectiveness of TransVFC across multiple downstream machine vision tasks of varying granularities.

## 2. Related Works

### 2.1. Neural Video Compression

Most of the existing neural video compression methods follow the motion-then-residual paradigm [6, 5, 18] and mainly include inter-prediction and residual (i.e. context) compression. Lu *et al.* [19] propose the first end-to-end video compression framework DVC which uses optical flow for inter-prediction and replaces the DCT transform with auto-encoder. Lu *et al.* [20] propose FVC to convert the video from the pixel domain to the feature domain and use deformable convolution for motion estimation and motion compensation in the feature domain. In traditional hybrid coding frameworks and above neural video compression frameworks, residuals are calculated based on mathematical subtraction. This method is simple and easy to implement, but it may not be the optimal solution for compression. Li *et al.* [21] redefine the concept of residual and transform subtraction-based residual into conditional residual calculated by the neural codec, named DCVC. Sheng *et al.* [22] propose DCVC-TCM with a multi-scale conditional residual, which enhances the ability to remove inter-frame temporal redundancy. Overall, existing neural video compression methods improve compression efficiency from various perspectives such as inter-prediction, residual compression, and entropy models. Many NVC methods (e.g., DCVC-series [6, 7, 5]) demonstrate formidable compression capabilities.

### 2.2. Neural-based Video Coding for Machines

The exploration of neural-based VCM unveils two pivotal paradigms: the Analyze-Then-Compress (ATC) and the Compress-Then-Analyze (CTA).

#### 2.2.1. Image and Video Compression in CTA Paradigm

With the surge in machine vision applications, the video compression framework is re-envisioned to better cater to downstream machine vision tasks. Some methods [23, 24] bridge the image codec and downstream task networks, then integrate the downstream task loss function to guide the optimization of the compression network, thus tailor-fitting it for enhanced performance on specific tasks. In addition, Tian *et al.* [11, 10] propose maintaining semantic similarity through an additional bitstream,

which improves the performance of multiple downstream tasks in an unsupervised way. Furthermore, the introduction of plug-and-play pre-processing modules [15] marks a significant advancement. These approaches achieve better downstream performance by enhancing important regions and filtering useless details for downstream analysis. Moreover, Video Coding for Machines is a sub-task of Video Coding for Humans and Machines. Some studies [3, 4, 25] modify the decoder and use features originally dedicated to fully reconstructing images, for downstream video analysis.

### 2.2.2. Feature Compression in ATC Paradigm

Intermediate feature compression is a widely studied VCM method under the ATC paradigm. Intermediate features contain more general information about images than high-level features and offer the potential for multi-task analysis. Moreover, they preserve the original spatial structure, which enables more effective redundancy removal through neural networks. Unlike shallow features, intermediate features undergo preliminary extraction, filtering out irrelevant information for machine vision tasks, making it easier to compress. In image feature compression, some approaches adopt traditional hybrid codec [26] or a VAE-based network optimized by feature distortion and specific task loss [27] for intra-compression. Moreover, some efforts [28, 29] change the compressed object from a single intermediate feature to the multi-scale features and compress them into a joint bit stream. In video features compression, Misra *et al.* [12] introduce an end-to-end feature compression network. It employs a simple ResBlock-based [30] bi-prediction in the feature domain and the entire framework is optimized for specific downstream tasks. Sheng *et al.* [14] propose a framework that conducts pixel-feature-domain inter-compression and supports multiple downstream tasks by freezing codec and optimizing downstream networks. However, there is a limitation to retraining and redeploying the upstream feature codec or whole downstream task networks in practical applications. In light of the above challenge, there's a growing need for adaptable and scalable VCM solutions.

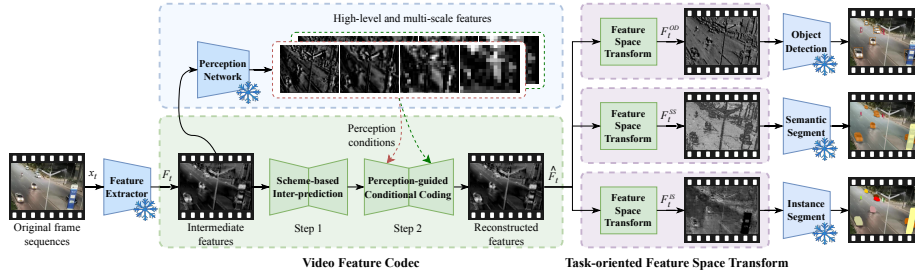


Figure 2: The overview of the proposed Transformable Video Feature Compression (TransVFC) framework.  $F_t^{OD}$ ,  $F_t^{SS}$ , and  $F_t^{IS}$  denote features for downstream object detection, semantic segmentation, and instance segmentation. The TransVFC framework employs a compress-then-transfer process. In detail, the codec conducts scheme-based inter-prediction to form a coarse compensated feature and then performs perception-guided conditional coding for fine reconstruction. Then, the reconstructed features are transferred to other feature spaces of diverse downstream machine vision tasks by Feature Space Transform (FST) modules. Notably, each downstream task corresponds to a distinct FST module.

### 3. Methodology

The pipeline of the proposed Transformable Video Feature Compression (TransVFC) framework is shown in Figure 2. It contains two main components: a neural-based video feature codec and diverse Feature Space Transform (FST) modules. Inspired by [12, 20], the intermediate features are extracted by the *res2* layers of the ResNet-50 backbone in Faster R-CNN [31], then the 256D features are converted into a 64D representation to squeeze channel redundancy. The video feature codec follows the motion-then-residual paradigm, it employs the scheme-based inter-prediction module to get the coarse motion-compensated feature and then uses the perception-guided conditional coding module for fine feature reconstruction. After that, the FST modules transfer the reconstructed intermediate feature  $\hat{F}_t$  to different feature spaces, making them suitable for various downstream machine vision tasks. Notably, each downstream task is associated with a dedicated FST module.

#### 3.1. Scheme-based Inter-prediction

As shown in Figure 3, temporal redundancy exists among repeated spatial structures, thus highlighting the need for redundancy removal by inter-prediction techniques. For inter-prediction in the feature domain, the deformable-based approach [20]

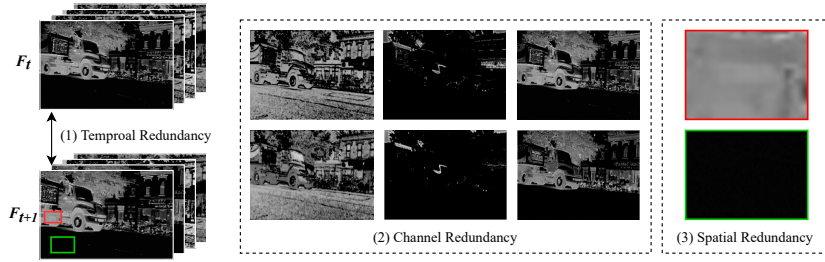


Figure 3: There are channel redundancy, temporal redundancy, and spatial redundancy among video features. The above redundancy needs to be squeezed by the video feature codec.

focuses on finding the optimal reference region and recombining existing feature values. To better address complex motion, we depart from this referencing-and-recombination method. Instead, we propose a scheme-based inter-prediction module. It generates a variety of potential motion schemes from reference frames and selectively combines them to get the compensated feature.

In the encoder, the Motion Estimation module performs four-step samplings for motion analysis across three distinct scales. The motion representation  $m_t$  contains both the global trends and the high-frequency details of motion, as shown in Figure 4(b). After that, the Motion Encoder compresses the  $m_t$  into a compact latent representation  $z$  with dimensions of  $(H/16, W/16, 64)$ . Subsequently, the latent representation  $z$  is quantized into  $\hat{z}$  for entropy coding and transmission. In the decoder, the motion combination matrix  $\hat{m}$  is reconstructed by the Motion Decoder module from  $\hat{z}$ . Leveraging the channel-wise computation by depthwise separable convolution [32], the Motion Compensation module generates diverse possible motion schemes based on the reference frame  $f_{ref}$ . Then, referring to the motion representation  $\hat{m}_t$ , schemes are judiciously selected and combined to form the compensated feature  $\tilde{f}_t$ . More analysis and visualization are shown in Section IV. The whole process of scheme-based inter-prediction is described in the following equation:

$$\tilde{f}_t = MC(f_{ref}, \mathcal{D}_m(\lfloor \mathcal{E}_m(ME(f_t, f_{ref})) \rfloor)) \quad (1)$$

where  $ME(\cdot)$  denotes Motion Estimation,  $MC(\cdot)$  denotes Motion Compensation.  $\mathcal{E}_m(\cdot)$  and  $\mathcal{D}_m(\cdot)$  denote Motion Encoder and Decoder, and  $\lfloor \cdot \rfloor$  is quantization operation.

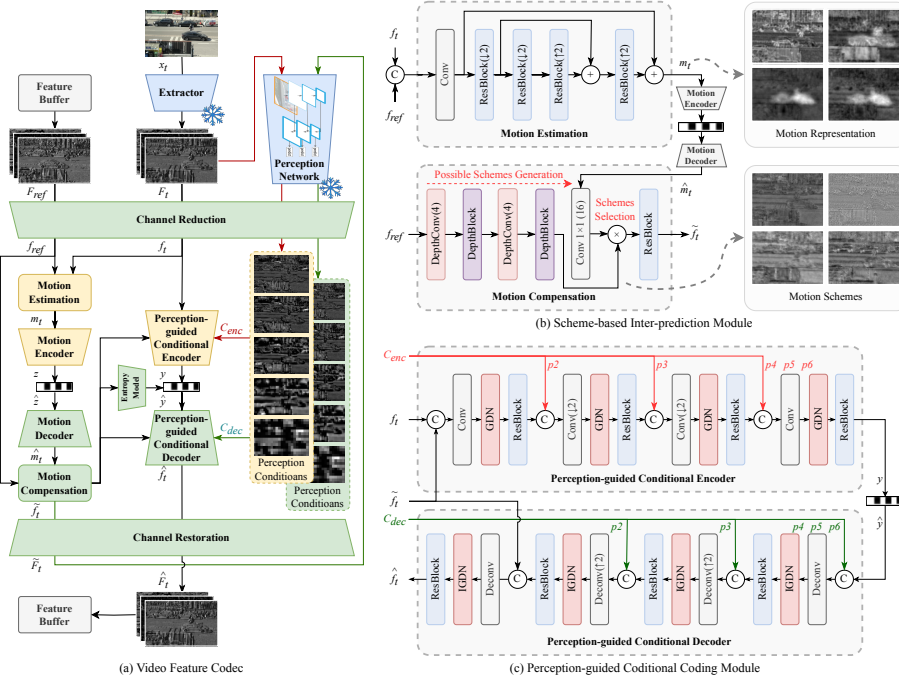


Figure 4: (a) The overall structure of the proposed neural-based video feature codec. It contains 3 main stages: channel reduction/restoration, scheme-based inter-prediction, and perception-guided conditional coding. The green modules are at both the encoder and decoder sides, while the yellow ones are only used at the encoder side. (b) The structure of the Scheme-based Inter-prediction module, including a Motion Estimation module, a Motion Compensation module, a Motion Encoder, and a Motion Decoder.  $DepthConv(n)$  represents a depthwise separable convolution layer with the number of channels increased by  $n$  times. The structure of  $DepthBlock$  is similar to  $ResBlock$  but replaces the convolution layers with the depthwise separable convolution layers. (c) The structure of the Perception-guided Conditional Encoder and Decoder. High-level and multi-scale features  $C_{enc}$  and  $C_{dec}$  are inferred from the Perception Network and used as conditions during residual compression and reconstruction.

### 3.2. Perception-guided Conditional Coding

The compensated feature  $\tilde{f}_i$  is obtained from the previous scheme-based inter-prediction. While, there is a gap in content detail between  $\tilde{f}_i$  and  $f_i$ , making it essential to complete the content details by the residual. We employ conditional coding to compress the residual in the feature domain. Since different machine vision tasks share common perception [33], we further introduce multi-scale high-level features Faster

R-CNN [31] as perception conditions to help the reconstructed features better align with downstream machine perception. Furthermore, the perception conditions offer TransVFC more prior knowledge during residual compression and reconstruction for lower entropy and better spatial redundancy removal, as follows:

$$H(f - \tilde{f}) > H(f|\tilde{f}) > H(f|\tilde{f}, C_{enc}, C_{dec}) \quad (2)$$

where  $H(\cdot)$  represents entropy,  $\tilde{f}$  denotes compensated feature,  $C_{enc}$  and  $C_{dec}$  denotes the perception condition for encoding and decoding, respectively.

As depicted in Figure 4(c), the Perception-guided Conditional Encoder comprises a four-step feature extraction process that compresses residuals into a compact and flat representation, while the decoder mirrors this structure symmetrically to reconstruct features. Multi-scale perception conditions are strategically inserted into positions that align with their corresponding shapes (specifically at 1/4, 1/8, and 1/16 scales), serving as conditions for both encoding and decoding to enhance the overall performance of the codec. Particularly, the encoding perception condition  $C_{enc} = \{p2, p3, p4, p5, p6\}$  are inferred from the original intermediate feature  $F_t$  by Feature Pyramid Network (FPN) backbone of Faster R-CNN. Due to the invisibility of  $F_t$  during decoding, the decoding perception condition  $C_{dec}$  is calculated from the compensated feature  $\tilde{F}_t$ . The whole process of perception-guided conditional coding is described as follows:

$$\hat{f}_i = \mathcal{D}_c(\mathcal{E}_c(f_i|C_{enc}, \tilde{f}_i)|C_{dec}, \tilde{f}_i) \quad (3)$$

where  $\mathcal{E}_c(\cdot)$  and  $\mathcal{D}_c(\cdot)$  denote Perception-guided Conditional Encoder and Decoder, respectively.

The latent representation  $y$  of residual with the dimension of  $(H/16, W/16, 96)$  is entropy-encoded by an entropy model similar to DCVC-TCM [22]. Regarding computational efficiency, auto-regressive or other complex techniques are not employed in the TransVFC. Additionally, a detailed explanation of how perception-guided conditional coding removes redundancy is in Section IV.

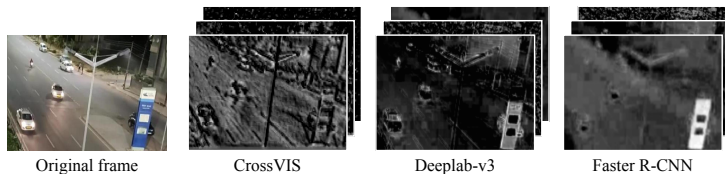


Figure 5: Visualizations of the first three channels of intermediate features across various machine vision networks. There are similar spatial structures but distinct feature patterns and textures among different intermediate features.

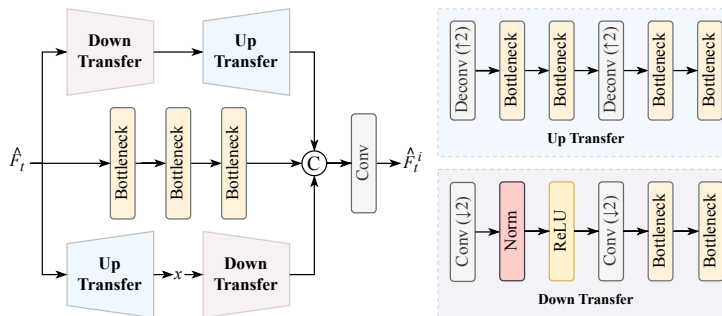


Figure 6: The structure of Feature Space Transform module. Reconstructed intermediate feature  $\hat{F}_t$  is transferred to  $\hat{F}_t^i$  in a new feature space for the  $i$ -th downstream machine vision task.

### 3.3. Task-oriented Feature Space Transform

Due to the gap between the intermediate features of different neural networks, as shown in Figure 5, the decoded video features can not be directly used in diverse downstream tasks. Some researches [3, 14] have already shown that intermediate features have the potential to be converted and used in other machine vision tasks. Inspired by [3], we design the multi-scale Feature Space Transform (FST) module that maps the reconstructed features to other feature spaces for different downstream tasks. Different from the existing neural-based VCM strategies [14, 12], our approach does not fine-tune the upstream feature codec and downstream task networks. Instead, it only requires training a single lightweight FST module for a specific downstream task.

As shown in Figure 6, the FST module is structured with three branches: the up-then-down branch, which coarsely reconstructs current frame  $\hat{x}_t$  for content preservation in pixel domain; the bottleneck-resblock [30] branch, facilitating feature migration

at the original shape; and the down-then-up branch, focusing on global information extraction. Additionally, a convolution layer is used to align the channel and spatial shape of the output features to the specific downstream task. The process of feature space transform is described below:

$$\hat{F}_t^i = FST^i(\hat{F}_t) \quad (4)$$

where  $FST^i(\cdot)$  denotes the  $i$ -th FST module,  $\hat{F}_t$  denotes the intermediate feature reconstructed by video feature codec, and  $\hat{F}_t^i$  denotes the transferred feature suitable for the  $i$ -th downstream task.

### 3.4. Optimization

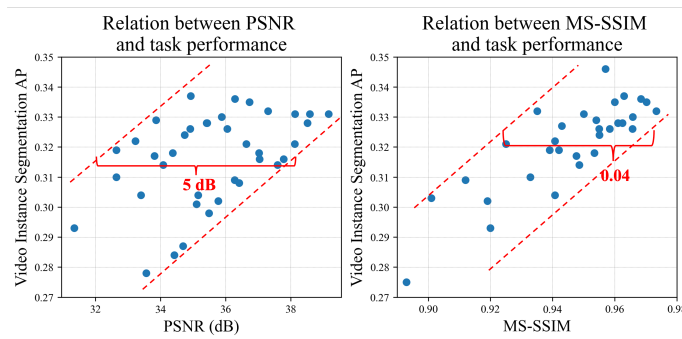


Figure 7: The correlation between the pixel-domain and HVS-related distortion metric (PSNR and MS-SSIM) and downstream machine vision performance (e.g., Average Precision of video instance segmentation) is weak. Optimizing the compression network for pixel-domain HVS distortion is not the best approach for the VCM scenario. The degraded videos are collected from traditional hybrid codecs and neural-based codecs [9, 6, 7, 22, 21, 20]. Particularly, dataset Youtube-VIS 2019 and model CrossVIS [34] are used.

Since there is a lack of strong correlation between HVS-oriented pixel-domain metrics and machine vision performance, as mentioned in Figure 7. The optimization of our proposed TransVFC is mainly conducted in the feature domain and divided into two stages.

#### 3.4.1. Optimization of the Video Feature Codec

The Rate-Distortion Optimization (RDO) of the proposed video feature codec is performed in the feature domain. The loss function  $\mathcal{L}_{codec}$  is detailed as below:

$$\mathcal{L}_{codec} = \lambda_R(R_r + R_m) + \lambda_f D_f + \lambda_c D_c + \lambda_p D_p \quad (5)$$

where  $\lambda_R$ ,  $\lambda_f$ ,  $\lambda_c$ , and  $\lambda_p$  are coefficients for balancing different loss terms.  $R_r$  and  $R_m$  represent the bitrates of residual and motion representation.  $D_f$  denotes the Mean Square Error (MSE) between the original intermediate feature  $F_t$  and reconstructed feature  $\hat{F}_t$ .  $D_c$  denotes the MSE between  $F_t$  and compensated feature  $\tilde{F}_t$ .  $D_p$  denotes the distortion in perception space and is defined as follows:

$$D_p = \frac{1}{N} \sum_{j=1}^{N=5} MSE(PN_j(F_t), PN_j(\hat{F}_t)) \quad (6)$$

where  $PN(\cdot)$  shorts for the perception network in TransVFC, and  $N$  is the number of high-level output features from the perception network.

#### 3.4.2. Optimization of Feature Space Transform Module

Since the FST module mainly transforms the reconstructed intermediate features to other spaces for downstream networks. It is optimized for minimizing the downstream task loss and feature distortion in new feature space. All other modules are frozen in this training stage.

$$\mathcal{L}_{FST} = \lambda_{task} \mathcal{L}_{task} + \lambda_x D_x + \lambda_{mid} D_{mid} + \lambda_{high} D_{high} \quad (7)$$

where  $\lambda_{task}$ ,  $\lambda_x$ ,  $\lambda_{mid}$  and  $\lambda_{high}$  are coefficients for balancing different loss terms.  $\mathcal{L}_{task}$  is the loss of downstream task network.  $D_{mid}$  denotes MSE between transferred feature  $\hat{F}_t^i$  and original feature  $F_t^i$  for  $i$ -th downstream task,  $D_x$  denotes MSE between reconstructed frame  $\hat{x}_t$  and original frame  $x_t$ , and the definition of  $D_{high}$  is as follows:

$$D_{high} = \frac{1}{N} \sum_{j=1}^N MSE(TASK_j^i(F_t^i), TASK_j^i(\hat{F}_t^i)) \quad (8)$$

where  $TASK^i(\cdot)$  represents the backbone of the  $i$ -th downstream task network and  $N$  is the number of high-level output features in the  $i$ -th downstream backbone.

## 4. Experiment

### 4.1. Experimental Settings

#### 4.1.1. Downstream Machine Vision Tasks

The performance of TransVFC is verified on three downstream tasks of different granularities. We employ the CrossVIS [34] framework for video instance segmentation, Deeplab-v3 [35] for semantic segmentation, and Faster R-CNN [31] for object detection. Parameters of all downstream networks are frozen throughout the entire experiment.

#### 4.1.2. Datasets

Experiments are conducted on the YoutubeVIS2019 (YTVIS2019)[34] and Video Scene Parsing in the Wild (VSPW) [36] datasets. YTVIS2019 dataset is a large video dataset including 2,883 videos with frame-level annotations of 40 categories for video instance segmentation. The resolutions range from 1080P to 360P, and the data pre-process follows [34]. VSPW dataset is a large video dataset including 3,536 videos in 480P resolution across 231 scenarios. It has frame-level annotations of 124 categories for video semantic segmentation.

#### 4.1.3. Compared Methods

The proposed TransVFC is compared with traditional hybrid codecs VTM-23.1 (lowdelay-P) [17], HM-18.0 (lowdelay-P) <sup>1</sup> [37] and x265 (FFmpeg-4.2.7, zerolatency) <sup>2</sup> [38], and open-sourced neural video compression (NVC) frameworks, such as DCVC-DC [6], DCVC-HEM [7], DCVC-TCM [22], DCVC [21], and FVC [20].

---

<sup>1</sup>The command of VTM and HM is `./bin/TAppEncoderStatic -c ./cfg/encoder_lowdelay_P_main.cfg -i {input_path} -b {output_binary_path} -o {output_path} -wdt {width} -hgt {height} -q {QP} -fr {frame_rate} -InputChromaFormat=420 --IntraPeriod=12`

<sup>2</sup>The command of x265 is `FFREPORT=file=ffreport.log:level=56 ffmpeg -pix_fmt yuv420p -s {width}x{height} -i {input_path} -c:v libx265 -tune zerolatency -x265-params "crf={crf}:keyint=12:verbose=1" out.mkv`

For compared NVC methods, all available pre-trained models are evaluated across different metrics (PSNR, MS-SSIM, YUV), showcasing only the model with the highest rate-task performance. In addition, VCM-oriented video codec SMC++ [11] is used as a compared method. The VTM-23.1 serves as the anchor for calculating BD-Rate [39] (the lower BD-Rate means more bitrate saving).

#### 4.1.4. Implementation Details

Stages	$\mathcal{L}_{codec}$	Learning rate
1	$\frac{1}{2}\lambda_R R_y + \lambda_f D_f + \lambda_c D_c + \lambda_p D_p$	$1 \times 10^{-4}$
2	$\frac{1}{2}\lambda_R(R_y + R_z) + \lambda_f D_f + \lambda_c D_c + \lambda_p D_p$	$1 \times 10^{-4}$
3	$\lambda_R(R_y + R_z) + \lambda_f D_f + \lambda_c D_c + \lambda_p D_p$	$1 \times 10^{-4}$
4	$\lambda_R(R_y + R_z) + \lambda_f D_f + \lambda_c D_c + \lambda_p D_p$	$5 \times 10^{-5}$
5	$\lambda_R(R_y + R_z) + \lambda_f D_f + \lambda_c D_c + \lambda_p D_p$	$1 \times 10^{-5}$

Table 1: Training strategy for video feature codec

Downstream tasks	$\lambda_{mid}$	$\lambda_{high}$	$\lambda_x$	$\lambda_{task}$
Object detection	16	4	1024	10
Instance segmentation	8	64	1024	1
Semantic segmentation	16	64	1024	10

Table 2: Training hyperparameters  $\lambda$  for Feature Space Transform module

In the first stage, we optimize the video feature compression framework of different bitrates with  $\lambda_R = 16, 32, 128, 256$ ,  $\lambda_f = 16$ ,  $\lambda_c = 0.1\lambda_f$ , and  $\lambda_p = 4$ . The training strategy is shown in Table 1. The input features during training are cropped to  $128 \times 128$ . The neural-based video feature codec is optimized on the YTVIS2019-train.

In the second stage, different weights  $\lambda$  are used to train FST modules for each downstream task, as shown in the Table 2. Weights  $\lambda$  are determined to ensure that different loss items are in a similar order of magnitude and that the magnitudes of gradients produced by each loss item are approximately balanced, which achieves equilibrium across the multiple optimization objectives. The training iteration number of the FST module is  $100k$ , and the learning rate is set to  $1 \times 10^{-5}$ .

The implementation of TransVFC is based on PyTorch 1.9.0. The whole framework is optimized on a single NVIDIA RTX 3090 24GB with  $batchsize = 4$ .

	Object detection	Semantic segmentation	Instance segmentation
VTM-23.1 (low-delay) [17]	0.00	0.00	0.00
HM-18.0 (low-delay) [37]	7.82	<b>-11.40</b>	5.60
x265 (zero-latency) [38]	-1.16	36.34	3.91
FVC (CVPR'20) [20]	97.15	130.03	368.56
DCVC (NerulPS'21) [21]	50.34	286.38	109.43
DCVC-TCM (TMM'22) [22]	7.84	204.46	32.69
DCVC-HEM (ACMMM'22) [7]	-3.92	183.80	46.34
DCVC-DC (CVPR'23) [6]	-4.53	145.53	26.56
SMC++ (arXiv'24) [11]	-4.28	74.61	-6.77
TransVFC (Ours)	<b>-15.21</b>	63.60	<b>-27.67</b>

Table 3: BD-Rate (%) ↓ comparison. The anchor is VTM-23.1. **Bold** indicates the best results.

## 4.2. Rate-task Performance

### 4.2.1. Object Detection

The implementation of Faster R-CNN [31] is based on Detectron2 [40], which is an extensively used and efficient framework for keypoint detection, object detection, and segmentation. Following [31], Average Precision (AP)<sup>3</sup> is used to evaluate the performance of object detection. Figure 8(a) displays the performance across various bitrates. As shown in Table 3, in terms of rate-task performance, TransVFC achieves a 15.21% reduction in bitrate compared to VTM. From a rate-time perspective, TransVFC has a better speed-performance balance than other neural-based methods.

### 4.2.2. Semantic Segmentation

We implement the Deeplab-v3 [35] based on TorchVision-0.9.0. Following [35], mean Intersection over Union (mIoU) is used for evaluating the performance of semantic segmentation. As demonstrated in Table 3, TransVFC outperforms the best neural-based method SMC++ [11] in terms of rate-task performance. Also, TransVFC achieves the best speed-performance balance compared to other neural-based methods, as shown in Figure 8(b).

<sup>3</sup>IoU=0.50:0.95, area=all, maxDets=100

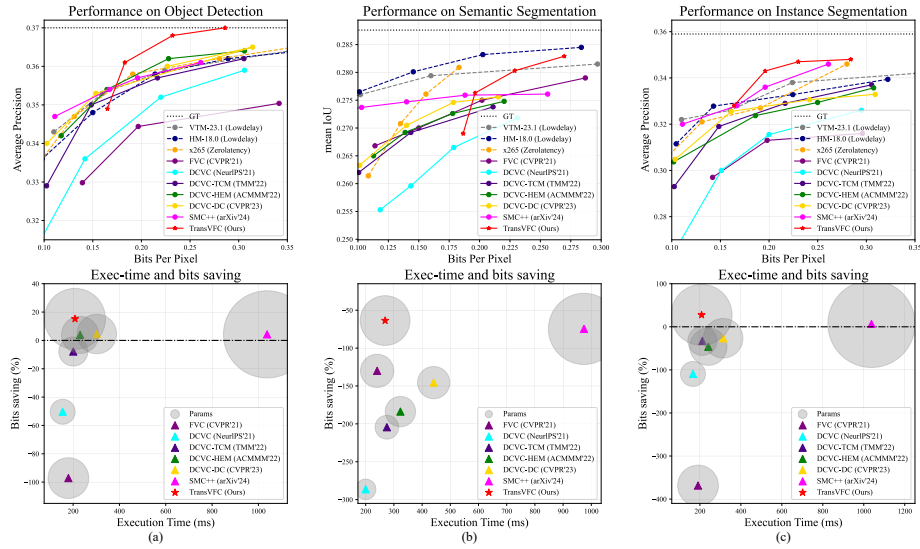


Figure 8: Rate-task performance of all compared methods (the upper row) and execution time of neural-based methods (the lower row) on object detection, semantic segmentation, and instance segmentation. The execution time including compression and downstream analysis was evaluated with  $batchsize = 1$  on a single NVIDIA RTX 3090 24GB, excluding the time of file I/O.

#### 4.2.3. Instance Segmentation

The CrossVIS is implemented on its official released code. Following [34], AP is the evaluation metric for video instance segmentation. As demonstrated in Table 3, in terms of rate task performance, TransVFC achieves the highest compression ratio, saving 27.67% of the bitrate compared to VTM. In terms of execution speed, compared to the high-performance NVC method DCVC-DC [6], TransVFC has a 34% faster execution speed, as shown in Figure 8(c).

As shown in Figure 9, TransVFC achieves better subjective segmentation results at different bitrates. Despite the high quality of reconstructed frames, the downstream task network CrossVIS struggles with maintaining the segmentation consistency of the main objects (e.g., the skateboard and the man holding an umbrella), often incorrectly segmenting them into multiple instances. In contrast, our framework better keeps the consistency of the instance and maximally retains the original segmentation results.

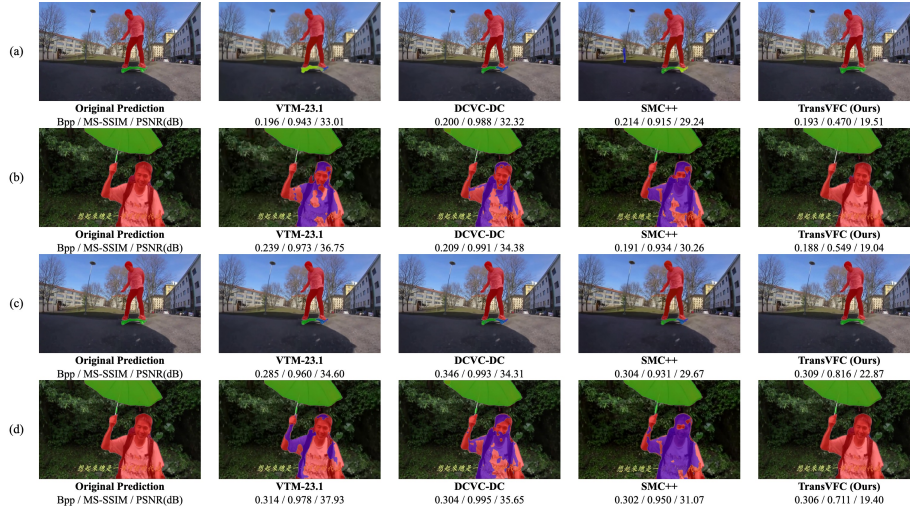


Figure 9: The visualization of predicted masks, bpp, MS-SSIM, and PSNR at low bitrates (a, b) and high bitrates (c, d). In videos with intense motion (a, c) and tiny movement (b, d), TransVFC maintains the original prediction and ensures consistency of the instance. The visualization shows that even if the reconstructed frames have high reconstruction quality, they may still underperform in downstream tasks.

### 4.3. Analysis

#### 4.3.1. Complexity of Video Features Compression

	Non-stream	With bitstream		Model params	MACs per pixel
	inference	Encoding	Decoding		
FVC (CVPR'20) [20]	165.8	/	/	21.0M	/
DCVC (NerulPS'21) [21]	129.1	1818.9	4738.3	7.9M	1.09M
DCVC-TCM (TMM'22) [22]	197.6	232.8	121.4	10.7M	1.40M
DCVC-HEM (ACMMM'22) [7]	240.6	250.3	124.6	17.5M	1.58M
DCVC-DC (CVPR'23) [6]	347.5	285.5	243.8	19.8M	1.27M
SMC++ (arXiv'24) [11]	830.1	/	/	96.2M	
TransVFC (Ours)	191.2	234.5	122.5	22.4+26.7M	1.16M

Table 4: Execution time (ms) on 720P frame, number of model parameters, and MACs per pixel of neural-based methods.

As shown in Table 4, we compared the execution time, parameter number, and MACs of our proposed video feature codec with other neural-based compression methods [20, 21, 22, 7, 6, 11]. Our proposed video feature codec consists of an optimized

codec with 22.4M parameters and a frozen perception network with 26.7M parameters. The inference time reflects the computation complexity of all neural-based modules on GPU without arithmetic coding. The encoding and decoding time includes the time for arithmetic coding operation but excludes file I/O. Although our codec has more parameters than other neural compression methods, it has fewer MACs per pixel than high-performance codecs like DCVC-DC and DCVC-HEM. The TransVFC has a better complexity-performance balance than other high-performance NVC approaches, with efficiency gains stemming from three aspects. Firstly, the intermediate features have a 1/4 spatial size of the original image, helping TransVFC use fewer convolutions and down/up-sampling operations than neural video compression frameworks. Secondly, to improve encoding and decoding speed, TransVFC uses a simple entropy model including a mean-scale hyperprior module and a temporal prior module [22], which is better parallelized. Thirdly, introducing depthwise convolution reduces computational complexity [6, 32], resulting in lower MACs.

#### 4.3.2. Complexity of Feature Space Transform

The FST module in the TransVFC framework is lightweight, with a parameter size of 4.3M. It is significantly smaller than the networks for downstream visual analysis (e.g., CrossVIS-ResNet50-version has 37.4M parameters), adding less additional training overhead. The execution time of feature space transform under 720P resolution is 11.7ms, which only accounts for 3.3% of the total time. The MACs per pixel of the FST module is 0.16M. The above results indicate that the FST module is highly effective during both training and inference stages.

#### 4.3.3. Visualization of Scheme-based Inter-prediction

Visualization of our proposed Scheme-based Inter-prediction module is shown in Figure 10. This module generates potential pattern schemes and then combines them by motion representation. The motion representation captures motion information, including local edge movements (e.g., channels 0 and 8) and large-scale motion (e.g., rapid movement of vehicles in channels 4 and 6). Meanwhile, motion schemes illustrate the potential components of the compensated feature, incorporating various types

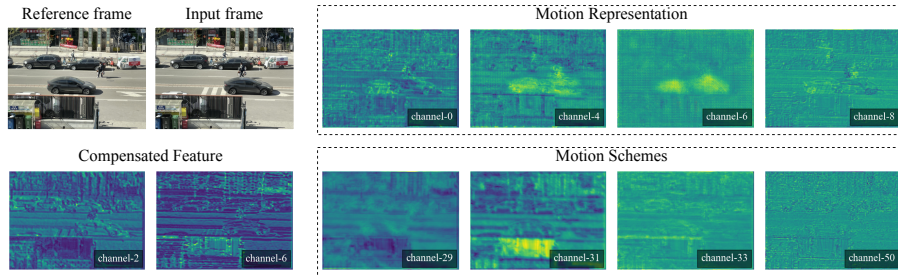


Figure 10: Visualization of compensated feature, motion representation, and motion schemes.

of pattern schemes. Subsequently, under the guidance of motion representation, these schemes are synthesized into the compensated feature.

The compensated feature is a coarsely reconstructed feature by inter-prediction and it is similar to the current feature. As shown in Figure 10, the feature of the car is already moved to a new position in the compensated frame. Since the compensated feature is just a coarse-version feature of the current frame, feature details is fulfilled by following conditional coding.

#### 4.3.4. Relation between Perception-guided Conditional Coding and Spatial Redundancy Removal

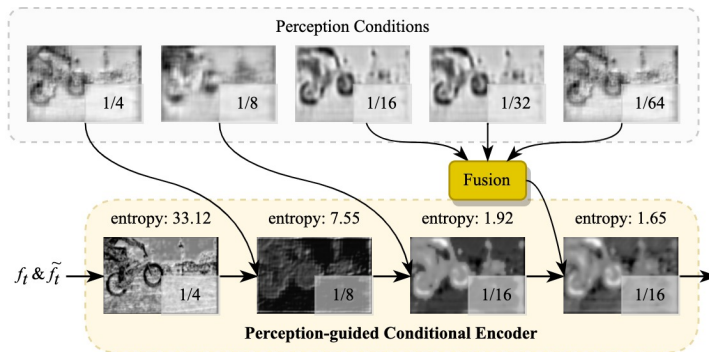


Figure 11: The process of perception-guided conditional encoding. The feature is compressed into a compact representation with lower entropy with the help of perception conditions as prior knowledge.

Spatial redundancy is prevalent in intermediate features, as adjacent regions often exhibit similar textures and high-frequency details, leading to overlapping or repeti-

tive information. The Perception-guided Conditional Coding module addresses this redundancy through two key perspectives: **Firstly**, as depicted in Figure 11, the original features are down-sampled multiple times and get smaller, compacter, and flatter. For a better understanding of the decrease of information, we take one frame as an example and calculate the entropy per pixel, as shown in equation 9. As dedicated in Figure 11, the feature’s entropy decreases during the encoding process, then the feature is compressed into a latent representation with lower entropy suitable for entropy coding and transmission. **Secondly**, the intermediate features to be compressed have significant spatial structural correlation and repetition with the perception condition. Since the perception condition (acting as prior knowledge) is already accessible on both encoder and decoder sides, there is no need to redundantly transmit this content from the encoder to the decoder. Instead, the decoder can effectively reconstruct the original content using the available perception information, further squeezing spatial redundancy and enhancing the efficiency of the coding process.

$$entropy = \sum_i^N p(f_i) \log(p(f_i)) / (H \times W) \quad (9)$$

where  $N$  is number of values in  $f_i$ ,  $p(\cdot)$  represents probability if each value,  $H$  and  $W$  is height and width of current frame. The feature  $f$  is 8-bit quantized for probability statistics.

#### 4.4. Ablation Study

Ablation experiments are conducted on the task of video instance segmentation and the model of CrossVIS [34].

##### 4.4.1. Video Feature Codec

To verify the effectiveness of the proposed scheme-based inter-prediction, our proposed Motion Estimation and Motion Compensation modules are replaced with existing deformable-based approach [20] as Model 1 in Table 5, which results in an 11.37% average bitrate increase. To verify the effectiveness of the perception conditions, we retain the framework structure but without using  $C_{enc}$  and  $C_{dec}$  as conditions, named Model 2. It is demonstrated that reconstructing video features without

Models	Scheme-based Inter-prediction	Perception condition	Perception loss	BD-Rate (%)↓
Model 1	✗	✓	✓	+11.37
Model 2	✓	✗	✓	+13.85
Model 3	✓	✓	✗	+36.92
Model 4	✓	✗	✗	+40.18
Model 5	✗	✗	✗	+46.71

Table 5: Ablation study on our proposed components in feature codec.

conditions causes a 13.85% bitrate increase. Furthermore, the high-level perception loss  $D_p$  is removed in Model 3, resulting in a 36.92% bitrate increase. The result of model 4 indicates that introducing high-level perception in both conditional coding and loss function can significantly boost the rate-task performance, 40.18% in total. Additionally, when both Scheme-based Inter-prediction and Perception-guided Conditional Coding are removed (Model 5), simplifying the codec to a structure similar to FVC [20] with deformable-based inter-prediction and residual coding, the bitrate increases by 46.71%.

#### 4.4.2. Feature Space Transform Module

Models	Bottleneck	Down-up	Up-down	BD-rate(%)↓
Model 6	✓	✓	✗	+2.83
Model 7	✓	✗	✓	+2.69
Model 8	✓	✗	✗	+5.69

Table 6: Ablation study on our proposed FST module.

To verify the function of each branch in the FST module, we removed the up-down branch (model 6), the down-up branch (model 7), and both branches (model 8), as shown in Table 6. The experimental results demonstrate that each branch plays a significant role in the quality of feature space transformation. Notably, the up-down branch enhances feature-domain transformation by coarsely reconstructing the original image, making the FST module aware of pixel-domain content, as illustrated in Figure 12.

Additionally, we conduct an ablation study on the complexity of the FST module.



Figure 12: Visualization of up-sampled results. The “up-then-down” branch can coarsely reconstruct the original content in the pixel domain, which helps the feature transfer process get a knowledge of pixel-domain content.

We roughly double the number of parameters of the FST. The number of parameters in FST increases from 4.30M to 5.92M (+37%), and the MACs per pixel rise from 0.14M to 0.26M (+86%). The FST only further reduces the BD-Rate by 2.42%. We also roughly reduce the number of res-blocks. The number of parameters reduces to 3.53M and MACs per pixel reduces to 0.12M. The BD-Rate increases by 5.60%. It shows that the current structure is appropriate since more complexity will only bring limited BD-rate reduction.

#### 4.4.3. Comparison of Different Approaches in ATC Paradigm

Models	Codec	Task	BD-Rate(%)↓	Optimized params	GPU mem (GiB)	Training time per step (s)
Model 9	✓	✗	-6.33	22.4M	19.3(+12.9%)	1.430(+14.1%)
Model 10	✗	✓	-7.16	37.4M	18.6(+8.8%)	1.374(+9.7%)
Ours	✗	✗	0	4.3M	17.1	1.253

Table 7: Ablation study on different approaches in ATC paradigm. “✓” means optimized and “✗” means frozen.

Other ATC-based VCM pipelines are implemented based on TransVFC, as detailed in 7. Referring to [12, 13, 14], we fine-tune either the upstream video feature codec (model 9) or the downstream task network (model 10) instead of the FST module. Experimental results indicate that training either the upstream or the downstream network leads to additional bitrates saving. However, this comes at the cost of optimizing more

parameters, consuming more computational resources and training time. Benefiting from the FST module, our approach uses fewer computational resources and avoids redeploying the upstream video feature codec or downstream task networks, offering better scalability.

#### 4.4.4. Influence on I-frame Codec

The proposed TransVFC directly uses the feature of the first lossless frame and calculates the bits per pixel (bpp) of its original I-frame jpeg file. Additionally, our experiments show that introducing x265 for I-frames compression causes a 5.10% bitrate increase.

## 5. Conclusion

We have proposed a Transformable Video Feature Compression (TransVFC) framework. It offers a scalable solution for multi-task VCM scenarios and eliminates the need for fine-tuning the upstream codec and downstream machine vision tasks. We devised a novel neural-based video feature codec to achieve continuous feature compression, which incorporates a scheme-based inter-prediction module for feature-domain temporal redundancy squeezing and employs perception-guided conditional coding to make features better align with machine perception. We designed the Feature Space Transform module to transfer intermediate features to multiple downstream tasks effectively. Experiments are conducted on three downstream machine vision tasks of different granularities, demonstrating that TransVFC delivers promising compression efficiency and scalability.

Despite the promising results, our approach has limitations. Its performance tends to decrease in low-bitrate scenarios. The decrease may stem from challenges in inter-prediction when dealing with low-quality features, which introduces cumulative error in the feature domain and affects overall rate-task performance. Meanwhile, there remains a gap between our framework and real-time systems such as FFmpeg [38]. Our future work aims to improve performance in low-bitrate conditions, reduce coding latency, and introduce new technology like the variable-bitrate mechanism.

We hope that our approach can inspire advancements in video feature compression for multi-task scenarios and contribute to the development of the ATC-based VCM.

## 6. Acknowledgements

This work is supported by the Fundamental Research Funds for the Central Universities (2024JBZX001), the National Natural Science Foundation of China (62120106009, 62372036, U24B20179).

## 7. Declaration of generative AI and AI-assisted technologies in the writing process.

During the preparation of this work, the author(s) used ChatGPT to polish the manuscript and enhance its readability. After using this tool/service, the author(s) reviewed and edited the content as needed and take(s) full responsibility for the content of the published article.

## References

- [1] R. M. A. Pandeewari, G. Rajakumar, Deep intelligent technique for person re-identification system in surveillance images, *Pattern Recognition* 162 (2025) 111349. doi:<https://doi.org/10.1016/j.patcog.2025.111349>.
- [2] X. Liu, L. Jin, X. Han, J. You, Mutual information regularized identity-aware facial expression recognition in compressed video, *Pattern Recognition* 119 (2021) 108105.
- [3] H. Choi, I. V. Bajić, Scalable image coding for humans and machines, *IEEE Transactions on Image Processing* 31 (2022) 2739–2754. doi:[10.1109/TIP.2022.3160602](https://doi.org/10.1109/TIP.2022.3160602).
- [4] E. Özyılkan, M. Ulhaq, H. Choi, F. Racapé, Learned disentangled latent representations for scalable image coding for humans and machines, in: *Proceedings of Data Compression Conference (DCC)*, 2023, pp. 42–51.

- [5] J. Li, B. Li, Y. Lu, Neural video compression with feature modulation, in: Proceedings of the IEEE/CVF Conference on Computer Vision and Pattern Recognition (CVPR), 2024, pp. 26099–26108.
- [6] J. Li, B. Li, Y. Lu, Neural video compression with diverse contexts, in: Proceedings of the IEEE/CVF Conference on Computer Vision and Pattern Recognition (CVPR), 2023, pp. 22616–22626.
- [7] J. Li, B. Li, Y. Lu, Hybrid spatial-temporal entropy modeling for neural video compression, in: Proceedings of the ACM International Conference on Multimedia, 2022, pp. 1503–1511.
- [8] T. Wiegand, G. J. Sullivan, G. Bjontegaard, A. Luthra, Overview of the H.264/AVC video coding standard, *IEEE Transactions on circuits and systems for video technology* 13 (7) (2003) 560–576.
- [9] A. Abramowski, Towards H.265 video coding standard, in: Proceedings of Photonics Applications in Astronomy, Communications, Industry, and High-Energy Physics Experiments, Vol. 8008, SPIE, 2011, pp. 387–393.
- [10] Y. Tian, G. Lu, G. Zhai, Z. Gao, Non-semantics suppressed mask learning for unsupervised video semantic compression, in: Proceedings of the IEEE/CVF International Conference on Computer Vision (ICCV), 2023, pp. 13610–13622.
- [11] Y. Tian, G. Lu, G. Zhai, SMC++: Masked learning of unsupervised video semantic compression, *arXiv preprint arXiv:2406.04765* (2024).
- [12] K. Misra, T. Ji, A. Segall, F. Bossen, Video feature compression for machine tasks, in: Proceedings of the IEEE International Conference on Multimedia and Expo (ICME), 2022, pp. 1–6.
- [13] J. Shao, J. Zhang, Bottleneck++: An end-to-end approach for feature compression in device-edge co-inference systems, in: Proceedings of IEEE International Conference on Communications Workshops (ICC Workshops), 2020, pp. 1–6.

- [14] X. Sheng, L. Li, D. Liu, H. Li, VNVC: A versatile neural video coding framework for efficient human-machine vision, *IEEE Transactions on Pattern Analysis and Machine Intelligence* (2024).
- [15] M. Yang, F. Yang, L. Murn, M. G. Blanch, J. Sock, S. Wan, F. Yang, L. Heranz, Task-switchable pre-processor for image compression for multiple machine vision tasks, *IEEE Transactions on Circuits and Systems for Video Technology* (2023). doi:10.1109/TCSVT.2023.3348995.
- [16] M. Yamazaki, Y. Kora, T. Nakao, X. Lei, K. Yokoo, Deep feature compression using rate-distortion optimization guided autoencoder, in: *Proceedings of the IEEE International Conference on Image Processing (ICIP)*, 2022, pp. 1216–1220.
- [17] VTM-23.1, [https://vcgit.hhi.fraunhofer.de/jvet/WVCSsoftware\\_VTM](https://vcgit.hhi.fraunhofer.de/jvet/WVCSsoftware_VTM), accessed 2025-01-31 (2024).
- [18] C. Xu, M. Liu, C. Yao, W. Lin, Y. Zhao, IBVC: Interpolation-driven b-frame video compression, *Pattern Recognition* 153 (2024) 110465.
- [19] G. Lu, W. Ouyang, D. Xu, X. Zhang, C. Cai, Z. Gao, DVC: An end-to-end deep video compression framework, in: *Proceedings of the IEEE/CVF Conference on Computer Vision and Pattern Recognition (CVPR)*, 2019, pp. 11006–11015.
- [20] Z. Hu, G. Lu, D. Xu, FVC: A new framework towards deep video compression in feature space, in: *Proceedings of the IEEE/CVF Conference on Computer Vision and Pattern Recognition (CVPR)*, 2021, pp. 1502–1511.
- [21] J. Li, B. Li, Y. Lu, Deep contextual video compression, *Advances in Neural Information Processing Systems (NeurIPS)* 34 (2021) 18114–18125.
- [22] X. Sheng, J. Li, B. Li, L. Li, D. Liu, Y. Lu, Temporal context mining for learned video compression, *IEEE Transactions on Multimedia* 25 (2023) 7311–7322.
- [23] L. D. Chamain, F. Racapé, J. Bégaint, A. Pushparaja, S. Feltman, End-to-end optimized image compression for machines, a study, in: *Proceedings of Data Compression Conference (DCC)*, 2021, pp. 163–172.

- [24] C. Gao, D. Liu, L. Li, F. Wu, Towards task-generic image compression: A study of semantics-oriented metrics, *IEEE Transactions on Multimedia* 25 (2023) 721–735. doi:10.1109/TMM.2021.3130754.
- [25] L. Liu, Z. Hu, Z. Chen, D. Xu, ICMH-Net: Neural image compression towards both machine vision and human vision, in: *Proceedings of the ACM International Conference on Multimedia*, 2023, pp. 8047–8056.
- [26] Z. Chen, K. Fan, S. Wang, L.-Y. Duan, W. Lin, A. Kot, Lossy intermediate deep learning feature compression and evaluation, in: *Proceedings of the ACM International Conference on Multimedia*, 2019, pp. 2414–2422.
- [27] W. Yang, H. Huang, Y. Hu, L. Duan, J. Liu, Video coding for machines: Compact visual representation compression for intelligent collaborative analytics, *IEEE Transactions on Pattern Analysis and Machine Intelligence* (01) (2024) 1–18.
- [28] Z. Zhang, M. Wang, M. Ma, J. Li, X. Fan, MSFC: Deep feature compression in multi-task network, in: *Proceedings IEEE International Conference on Multimedia and Expo (ICME)*, 2021, pp. 1–6.
- [29] Y. Kim, H. Jeong, J. Yu, Y. Kim, J. Lee, S. Y. Jeong, H. Y. Kim, End-to-end learnable multi-scale feature compression for VCM, *IEEE Transactions on Circuits and Systems for Video Technology* (2023).
- [30] K. He, X. Zhang, S. Ren, J. Sun, Deep residual learning for image recognition, in: *Proceedings of the IEEE/CVF Conference on Computer Vision and Pattern Recognition (CVPR)*, 2016, pp. 770–778.
- [31] R. Gavrilescu, C. Zet, C. Foşalău, M. Skoczylas, D. Cotovanu, Faster R-CNN: an approach to real-time object detection, in: *Proceedings of the International Conference and Exposition on Electrical And Power Engineering (EPE)*, 2018, pp. 0165–0168. doi:10.1109/ICEPE.2018.8559776.
- [32] F. Chollet, Xception: Deep learning with depthwise separable convolutions, in: *Proceedings of the IEEE/CVF Conference on Computer Vision and Pattern Recognition (CVPR)*, 2017, pp. 1251–1258.

- [33] X. Zou, Z.-Y. Dou, J. Yang, Z. Gan, L. Li, C. Li, X. Dai, H. Behl, J. Wang, L. Yuan, et al., Generalized decoding for pixel, image, and language, in: Proceedings of the IEEE/CVF Conference on Computer Vision and Pattern Recognition (CVPR), 2023, pp. 15116–15127.
- [34] S. Yang, Y. Fang, X. Wang, Y. Li, C. Fang, Y. Shan, B. Feng, W. Liu, Crossover learning for fast online video instance segmentation, in: Proceedings of the IEEE/CVF International Conference on Computer Vision (ICCV), 2021, pp. 8043–8052.
- [35] S. C. Yurtkulu, Y. H. Şahin, G. Unal, Semantic segmentation with extended DeepLabv3 architecture, in: Proceedings of the IEEE Conference on Signal Processing and Communications Applications (SIU), 2019, pp. 1–4.
- [36] J. Miao, Y. Wei, Y. Wu, C. Liang, G. Li, Y. Yang, VSPW: A large-scale dataset for video scene parsing in the wild, in: Proceedings of the IEEE/CVF Conference on Computer Vision and Pattern Recognition (CVPR), 2021, pp. 4133–4143.
- [37] HM-18.0, <https://vcgit.hhi.fraunhofer.de/jvet/HM>, accessed 2025-01-31 (2023).
- [38] FFmpeg, <https://github.com/FFmpeg/>, accessed 2025-01-31 (2023).
- [39] N. Barman, M. G. Martini, Y. Reznik, Revisiting Bjontegaard delta bitrate (BD-BR) computation for codec compression efficiency comparison, in: Proceedings of the Mile-High Video Conference, 2022, pp. 113–114.
- [40] Y. Wu, A. Kirillov, F. Massa, W.-Y. Lo, R. Girshick, Detectron2, <https://github.com/facebookresearch/detectron2> (2019).